Pattern Recognition Letters 33 (2012) 2065–2070

Contents lists available at SciVerse ScienceDirect

Pattern Recognition Letters

journal homepage: www.elsevier.com/locate/patrec

Self-adaptive evolutionary image registration using differential evolution and artificial immune systems ☆

José Santamaría [a,*], Sergio Damas [b], José M. García-Torres [c], Oscar Cordón [b,c,d]

[a] Dept. of Computer Science, University of Jaén, Spain
[b] European Centre for Soft Computing, Mieres, Spain
[c] Dept. of Computer Science and Artificial Intelligence, University of Granada, Spain
[d] Centro de Investigación en Tecnologías de La Información y de las Comunicaciones (CITIC-UGR), University of Granada, Spain

ARTICLE INFO

Article history:
Received 14 December 2011
Available online 13 July 2012

Communicated by G. Borgefors

Keywords:
Image registration
3D modeling
Evolutionary image registration
Self-adaptive

ABSTRACT

Image registration is present in many computer vision and computer graphics real-world applications. Specifically, it plays a crucial role within the 3D digital model acquisition pipeline, in which the iterative closest point (ICP) algorithm is considered the *de facto* standard for pair-wise alignment of range images. Nevertheless, the success of ICP depends on several assumptions. A new family of registration techniques have been recently proposed based on evolutionary computation paradigm to solve the common ICP problems.

Unlike previous contributions, we propose a novel self-adaptive evolutionary image registration algorithm able to search for the values of both the control and the problem solving parameters to achieve accurate alignments, simultaneously. It combines two different population-based optimization approaches that are concerned with the proper optimization of the control parameters and the image alignments, respectively. The performance of our proposal is compared with several state-of-the-art image registration methods.

1. Introduction

Image registration (IR) (Zitová and Flusser, 2003) is a fundamental task in the computer vision (CV) and computer graphics (CG) fields. It is aimed at finding either a spatial *transformation* (e.g. rotation, translation, etc.) or a correspondence (matching of similar image features) among two or more images acquired under different conditions: at different times, using different sensors, from different viewpoints, or a combination of them. IR aims to achieve the best possible overlapping transforming those independent images into a common one. Over the years, IR has been applied to tackle many real-world problems ranging from remote sensing to medical imaging, artificial vision, and computer-aided design (CAD). Likewise, different techniques facing the IR problem have been studied resulting in a large body of research. Several recent contributions reviewing the state of the art on IR methods can be found in (Santamaría et al., 2011; Salvi et al., 2007; Damas et al., 2011; Zitová and Flusser, 2003).

In the last few years, there is a growing interest in techniques to build high-quality 3D models of real-world objects and scenes acquired by range scanners (Bernardini and Rushmeier, 2002). Furthermore, such techniques should not require humans to manually produce those models using laborious and error-prone CAD-based approaches (Campbell and Flynn, 2001). Usually, the iterative closest point (ICP) algorithm (Besl and McKay, 1992; Chen and Medioni, 1992) is the *de facto* standard in pair-wise IR of range images, also named pair-wise range IR (RIR). However, this sort of methods are based on a classical optimization scheme (i.e. solution estimation using the least squares approach) and they rely on important assumptions to guarantee convergence to the optimal solution. In particular, they assume a near-optimal pose estimation[1] is initially provided. Otherwise, the IR process will be likely trapped in local optima (Rusinkiewicz et al., 2001).

Unlike the previous approaches, *approximate* or *heuristic* optimization methods (also named as *meta-heuristics* (Glover et al., 2003)) are able to achieve good quality outcomes for complex optimization problems. This optimization paradigm has introduced an

☆ This work is partially supported by both the Spanish Ministerio de Educación y Ciencia (Ref. TIN2009-07727) including European Development Regional Funds and the University of Jaén (Ref. R1/12/2010/61) including fundings from *Caja Rural de Jaén*.

* Corresponding author.
E-mail addresses: jslopez@ujaen.es (J. Santamaría), sergio.damas@softcomputing.es (S. Damas), jmgt@ugr.es (J.M. García-Torres), ocordon@decsai.ugr.es (O. Cordón).

[1] In some acquisition scenarios, the object to be sensed is on a calibrated turn table which allows an accurate alignment of adjacent images using ICP-based IR algorithms (Campbell and Flynn, 2001).

0167-8655/$ - see front matter © 2012 Elsevier B.V. All rights reserved.
http://dx.doi.org/10.1016/j.patrec.2012.07.002

outstanding interest in the IR community in the last decade, in which evolutionary computation (EC) (Bäck and Fogel, 1997) has provided successful outcomes. Unlike ICP-based algorithms, the latter variants do not require an accurate initial estimation of the pose. A recent experimental review of evolutionary IR methods applied to 3D modeling is to be find in (Santamaría et al., 2011).

Nevertheless, one of the main shortcomings of evolutionary algorithms (EAs) (Z. Michalewicz et al., 1996) is the need of a careful tuning of their control parameters (e.g. probability of mutation or crossover) in order to achieve the best (biased) performance. Determining appropriate control parameters is a time-consuming task that is usually carried out by hand in a trial-and-error way. Hence, the automatic or self-adaptive tuning of the EA control parameters is one of the most challenging problems in this field. In the last few years, many self-adaptive proposals have been contributed in the specific literature of EC (Eiben and Smith, 2011). However, we found that there is a lack of work done in application areas such as CV and CG. Thus, we propose a novel IR method based on EAs which adopts a self-adaptive scheme of the control parameters, we named StEvO. Our specific design of StEvO takes advantage of the synergy between two recent EAs: differential evolution (DE) (Storn, 1997) and artificial immune systems (AIS) (de Castro et al., 2002). We will accomplish an experimental study on the performance of this method facing the 3D reconstruction of real-world objects acquired by laser range scanners. We will compare our proposal with other state-of-the-art EAs using several range image datasets from the well-known SAMPL repository.

The structure of this paper is as follows. First, Section 2 introduces some basis on the IR problem of range data and the application of evolutionary principles to tackle it. Our self-adapted EA is described in Section 3. In Section 4, an experimental study is performed considering our proposal and several evolutionary IR methods. Finally, some conclusions and future works are provided in Section 5.

2. Evolutionary image registration

Range scanners are able to capture 3D images, named range images, from different viewpoints of the sensed object. Every range image shows a partial view of the complete geometry of the object surface. Thus, it is necessary to consider a reconstruction technique to perform the accurate integration of all the images by using RIR algorithms in order to achieve a complete and reliable model of the physical object. This framework is usually called 3D model reconstruction (Bernardini and Rushmeier, 2002).

There is not a universal design for a hypothetical IR method, since various considerations on the particular application must be taken into account (Zitová and Flusser, 2003). However, IR methods usually require the following four components: two input Images named as Scene $I_s = \{\vec{p}_1, \vec{p}_2, \ldots, \vec{p}_n\}$ and Model $I_m = \{\vec{p}'_1, \vec{p}'_2, \ldots, \vec{p}'_m\}$, with $\vec{p}_i$ and $\vec{p}'_j$ being image points; a Registration transformation f, being a parametric function relating the two images; a Similarity metric function F, in order to measure a qualitative value of closeness or degree of fitting between the transformed scene image, noted $f'(I_s)$, and the model image; and an Optimizer that looks for the optimal transformation f inside the defined solution search space.

Specifically, the optimizer is a crucial component for the success of the IR method. Since the ICP algorithm was introduced, many contributions have been proposed extending and partially solving the shortcomings of the original method, e.g. convergence to local minima (Feldmar and Ayache, 1996; Zhang, 1994; Rusinkiewicz et al., 2001). Nevertheless, they still assume that an initial near-optimal alignment of images is provided. Unlike the latter, EC-based IR algorithms have demonstrated their ability tackling complex optimization problems, e.g. in CV (Cordón et al., 2006; Perez et al., 2010; Yang et al., 2010). In particular, there is an increasing interest on applying EAs to the IR problem due to their capability to scape from local optima solutions (Santamaría et al., 2011; Damas et al., 2011).

As said, the 3D model reconstruction pipeline involves several pair-wise RIR steps (Bernardini and Rushmeier, 2002). Therefore, the application of every IR method aims to find the Euclidean motion that brings the *scene* view (I_s) into the best possible alignment with the *model* view (I_m). Such an Euclidean motion is given by a 3D rigid transformation (f) determined by six or seven real-coded parameters depending on using either Euler or axis plus angle representation for rotation, respectively. Specifically, we used the latter scheme. Thus, we define the rigid transformation as: a rotation $R = (\theta,\ Axis_x, Axis_y, Axis_z)$ and a translation $\vec{t} = (t_x, t_y, t_z)$, with θ and $\vec{Axis}$ being the angle and axis of rotation, respectively. The *scene* view consists of n points that are transformed as follows:

$$f(\vec{p}_i) = R(\vec{p}_i) + \vec{t}, \quad i = \{1, \ldots, n\} \tag{1}$$

Hence, pair-wise RIR can be formulated as an optimization problem devoted to search for the Euclidean transformation f^* achieving the best alignment of both $f(I_s)$ and I_m:

$$f^* = \arg\min_f F(I_s, I_m; f) \ s.t. : \ f^*(I_s) \cong I_m \tag{2}$$

according to the Similarity metric, F, being optimized. The median square error (MedSE) is a typical F function in 3D modeling (Santamaría et al., 2011) due to its robustness in the presence of outliers. MedSE can be formulated as follows:

$$F(I_s, I_m; f) = MedSE(d_i^2), \quad \forall i = \{1, \ldots, n\} \tag{3}$$

where $MedSE()$ corresponds to the median value of all the squared Euclidean distances, d_i^2, between the transformed scene point, $f(\vec{p}_i)$, and its corresponding closest point, $\vec{p}'_j$, in the *model* view I_m, that is:

$$d_i^2 = \|f(\vec{p}_i) - \vec{p}'_j\|^2, \quad j = \{1, \ldots, m\} \tag{4}$$

where m is the number of points of the I_m image. In order to speed up the computation of the closest point of every $f(\vec{p}_i)$ point, indexing structures as kd-trees (Silva et al., 2005) or the grid closest point (GCP) transform (Yamany et al., 1999) are often used.

3. Self-adapted evolutionary image registration

This section is devoted to describe our novel contribution based on an evolutionary optimization algorithm providing self-adaptive capabilities of the control parameters for facing pair-wise RIR problems.

3.1. Framework proposal

It is well-established in the EC community that the control parameters (e.g. the mutation and crossover probabilities, the tournament size of selection, etc.) have a strong influence on the behavior of EAs. Thus, parameter tuning has a potential of adjusting the optimization algorithm to the problem domain being solved. However, the election of the appropriate parameter values is a time-consuming task. Hence, the automatic control of the EA parameters is one of the most challenging tasks in the community of EC. In the last few years, many self-adaptive EA-based solutions have been proposed. A deeper analysis of these algorithms is out of the scope of this contribution and a broad study of this topic can be found in (Eiben and Smith, 2011). Among these, we found that the self-adaptive approach using the DE algorithm have shown improved performance (Brest et al., 2007).

Begin StEvO

1 $t \leftarrow 0$;
2 $\rho^{rand/1/bin}, \lambda^{rand/1/bin} \leftarrow 0$;
3 $\rho^{rand/1/exp}, \lambda^{rand/1/exp} \leftarrow 0$;
4 *InitiatePopulations* $(\Gamma_t, \Omega_t, \Upsilon_t)$;
5 *SortPopulation*$_{(F)}$ (Γ_t);
6 $x_{best} \leftarrow x_1$;
7 **While** (*Not reached stop criterion*) **Do**
8 **For** $i \leftarrow 1$ **to** l **Do**
9 Randomly select $r_1 \neq r_2 \neq r_3$ $(r_j \in \{1, \ldots, l\})$;
10 $x_{trial} \leftarrow SaBS\ (i, \Gamma_t, \Omega_t, r, \rho, \lambda)$;
11 **If** $(F(x_{trial}) < F(x_i))$ **Then**
12 $aff^{\varrho^i} \leftarrow \frac{F(x_i) - F(x_{trial})}{F(x_{trial})}$;
13 $x_i \leftarrow x_{trial}$;
14 **Else**
15 $aff^{\varrho^i} \leftarrow 0$;
16 **End-If**
17 **If** $(F(x_{trial}) < F(x_{best}))$ **Then**
18 $x_{best} \leftarrow x_{trial}$;
19 **End-If**
20 **End-For**
21 $\rho^{rand/1/bin} \leftarrow \frac{\lambda^{rand/1/bin}}{\lambda^{rand/1/bin} + \lambda^{rand/1/exp}}$;
22 $\rho^{rand/1/exp} \leftarrow \frac{\lambda^{rand/1/exp}}{\lambda^{rand/1/bin} + \lambda^{rand/1/exp}}$;
23 *TuningSaBSControlParameters* (Ω_t, Υ_t);
24 $t \leftarrow t + 1$;
25 **End-While**
26 **Return** x_{best};

End StEvO

Fig. 1. First-level pseudo-code of the StEvO algorithm.

Despite the previous, we found that there is a lack of application of this cutting-edge evolutionary techniques in real-world scenarios from the CV and CG fields, e.g. in IR. Thus, our contribution is twofold. On the one hand, we propose a new self-adaptive evolutionary optimization (StEvO) method for tackling RIR problems. On the other hand, we aim to achieve quality registration solutions as those obtained by the best evolutionary RIR methods of the state of the art. Thus, our proposed framework resembles the *meta-GA* (Mercer and Sampson, 1978) approach, being inspired in the cooperative design introduced in (Chunping and Xuefeng, 2009) which makes use of the DE algorithm.

The algorithmic description of StEvO is presented in Fig. 1. It can be structured in three main sections: *stage-0* (lines 1–7), *stage-1* (lines 8–22), and *stage-2* (line 23). First, both the registration solutions and the control parameters are randomly initialized using a uniform distribution in *stage-0*. Next, in the evolutionary optimization stage, *stage-1*, our new design of the DE algorithm searches for near-optimal registration solutions. Finally, *stage-2* makes use of the AIS algorithm in order to provide near-optimal values of the two control parameters of DE, i.e. ϱ^F and ϱ^{CR} (see Fig. 1). Then, the two linked optimization stages, i.e. *stage-1* and *stage-2*, iteratively co-operate using the same objective function (Eq. (3)). Therefore, the more suitable the control parameters are, the more accurate the registration solutions achieved will be.

At each iteration t of StEvO (see Fig. 1), each solution $x_i \in \Gamma$ $(\Gamma = \{x_1, x_2, \ldots, x_l\})$ is considered for possible replacement by a trial solution x_{trial} generated by using the DE algorithm (line 10). Unlike (Chunping and Xuefeng, 2009), our specific design makes use of a self-adaptive approach as introduced in (Qin et al., 2009). The proposed self-adaptive binary strategy (SaBS) considers a more reduced set of mutation and recombination operators than used in (Qin et al., 2009). Specifically, we followed the recommendations in (Qing et al., 2009) (see Section 6.1.1.4) and SaBS learns the best strategy between *rand*/1/*bin* and *rand*/1/*exp*. The learning scheme runs a probabilistic rule using the success rates $\rho^{rand/1/bin}$ and $\rho^{rand/1/exp}$. These are accordingly updated (lines 21 and 22) previous to run *stage-2* (line 23). The λ parameter refers to the number of times each strategy obtains an improved trial solution.

Initially, each 2-dimensional member $\varrho_i = \langle \varrho_i^F, \varrho_i^{CR} \rangle$ $(i = \{1, \ldots, l\})$ of both the antigens $\Omega = \{\varrho_1, \ldots, \varrho_l\}$ and the antibodies $\Upsilon = \{\varrho_1, \ldots, \varrho_{k=2 \cdot l}\}$ are randomly generated (line 4) previous to processing of *stage-2* using a Gaussian distribution $N(0, 1)$ and a uniform distribution $U[0, 1]$, respectively. At each iteration t of StEvO, the affinity score is computed in the *stage-1* each time a new improved trial solution is found. Otherwise the corresponding antigen $\varrho_i \in \Omega$ will be updated by 0 value (lines 12 and 15). Higher affinity values mean that the CS principle implemented in the *TuningSaBSControlParameters* procedure of *stage-2* obtained a better immune response, then matching more adapted control parameters with which *stage-1* will achieve improved RIR solutions.

A preliminary experiment was carried out aiming to analyze the robustness of StEvO using different values of the two AIS' control parameters: ϖ and β. As expected, we obtained the results reported in (Chunping and Xuefeng, 2009; Delibasis et al., 2011). In such references, AIS was also applied for tackling two different real-world optimization problems. In our study, both the AIS-based *stage-2* and the whole proposed framework (StEvO) achieved significant stable optimization outcomes with respect to the latter two control parameters for all the RIR problem instances considered. That behavior is not usual in the field of evolutionary IR (Santamaría et al., 2011). Typically, every evolutionary contribution needs a careful selection of the control parameters in order to achieve a successful performance. In this contribution, we considered the AIS' values in (Chunping and Xuefeng, 2009): $\varpi = 0.25$ and $\beta = 0.8$.

4. Experimental results

This section aims to present a number of experiments to study the robustness of the algorithms and the accuracy of the results obtained by the proposed self-adaptive optimization framework. As a benchmark, the results achieved by our StEvO-based RIR algorithm will be compared against those obtained by four state-of-the-art IR methods also using evolutionary approaches:

- Santamaria et al.'s proposal (Santamaria09) (Santamaría et al., 2009), a recent contribution based on the scatter search (SS) algorithm.
- de Falco et al.'s method (deFalco08) (de Falco et al., 2008), which makes use of a basic implementation of the DE algorithm.
- Silva et al.'s contribution (Silva05) (Silva et al., 2005), in which a steady-state GA variant is developed.
- Yamany et al.'s proposal (Yamany99) (Yamany et al., 1999), where the authors considered a binary representation of the transformation parameters and a canonical implementation of GAs.

A detailed description of these methods can be found in (Santamaría et al., 2011). The proposed algorithm[2] (StEvO) and the four

[2] The source code of the method is available in the website of the *Soft Computing and Intelligent Information Systems* Research Group (SCI2S, http://sci2s.ugr.es) of the University of Granada.

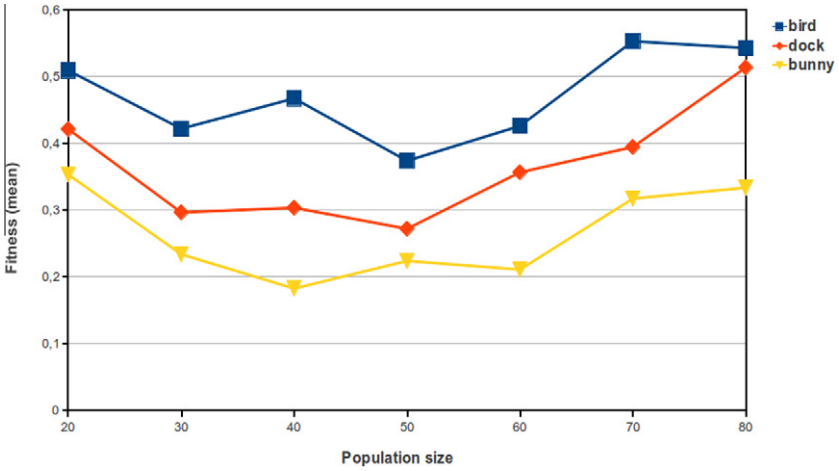

Fig. 2. Performance of the StEvO algorithm when facing the "Bird", "Dock", and "Bunny" datasets (forty degrees of overlapping RIR problem scenario) considering different population sizes.

compared RIR methods were implemented in C++ and compiled with the GNU/g++ tool. We adapted all the tested methods by using the same representation of the rigid transformation (f) and objective function (see Eq. (3) in Section 2) in order to accomplish a fair comparison. Other similarity metrics can be also used as objective function depending on the application.

4.1. Range image datasets and problem scenarios

In order to ease the comparison with the results reported in other contributions in the field (Salvi et al., 2007; Silva et al., 2005), our results correspond to a number of pair-wise RIR problem instances using different range datasets obtained from the well-known public repository of the Signal Analysis and Machine Perception Laboratory (SAMPL) of the Ohio State University. Specifically, we used six range datasets also considered in (Silva et al., 2005), named "Frog", "Bird", "Tele", "Lobster", "Angel", and "Buddha". Their size range from 8 K to 15 K.

Besides, we have considered several pair-wise RIR problem scenarios using two different overlapping degrees between pairs of adjacent images. Specifically, twenty and forty rotation degrees of the turn table were considered. Instead of considering feature-based approaches (Zitová and Flusser, 2003), we used a subsampled version of each range image in order to speed-up the computation of the objective function (see Eq. (3) in Section 2). In particular, five thousand points have been randomly chosen using a uniform distribution. Similar approaches were followed in other RIR proposals (Silva et al., 2005).

4.2. Parameter settings

In order to avoid execution bias, thirty different runs of each evolutionary RIR algorithm were performed. Every method tackled two kinds of problem scenarios: considering twenty and forty degrees of image overlapping. Moreover, all the tested algorithms start from an initial population of random solutions. In each run a rigid transformation is randomly generated using a uniform distribution and considering the following parameter ranges: each of the three rotation axis parameters will be in the range $[-1,1]$; the rotation angle will range in $[0^\circ, 360^\circ]$; and the range of three translation parameters is $[-40\text{ mm}, 40\text{ mm}]$. Such a random transformation is applied to the scene image $f_r(I_s)$ and the RIR method will search for the optimal transformation f^* between the proposed image $f_r(I_s)$ and the model image I_m. Note that this procedure provides an objective measure of the performance of the method. It will be based on the comparison of the transformation estimated by the method with the ground-truth given by the original location of the scene image, I_s.

Table 1
Statistical results of StEvO considering thirty different runs tackling the most complex scenario (forty degrees of overlapping). *RateBest* and *Dev.* columns show the percentage of times the best solution is found and the deviation with respect to the best mean fitness value achieved using 180 s, respectively.

	Bird		Dock		Bunny	
	RateBest (%)	Dev.	RateBest (%)	Dev.	RateBest (%)	Dev.
180 s	67	–	77	–	70	–
100 s	67	0	77	0	70	0
20 s	67	0.0008	47	0.0576	60	0.0185

We considered a fixed CPU time as the common stop criterion. All the methods were tested using different time limits in order to determine as a good threshold allowing all the methods to converge to good quality RIR solutions, and twenty seconds was the choice. Table 1 remarks the outcomes achieved by StEvO considering 180, 100, and 20 s. We can see how a reduced cpu time will achieve fast and accurate pair-wise RIR results.

All the pair-wise RIR methods were run on a PC with an Intel Pentium IV 2.6 MHz processor and 2 GB RAM. We considered the values of the control parameters of each of the four compared algorithms (Santamaria09, deFalco08, Yamany99, and Silva05) as those used in their original contribution. Regarding StEvO, we performed some preliminary experiments using different population sizes for the optimization procedure of the *stage-1*. Fig. 2 shows the performance (mean fitness value of thirteen runs) of StEvO considering twenty seconds run time and different population sizes. We found that the more stable and accurate results are around a population size of 50 solutions ($l = 50$).

Nevertheless, it is known that stable results will depend on the dimension of the optimization problem[3].

4.3. Analysis of results

Tables 1–3 show statistical results of the objective function F (see Eq. (3)) corresponding to the thirty runs carried out by each

[3] More information on the influence of the population size can be found in (Lobo et al., 2006).

Table 2
RIR results of the twenty degrees of overlapping problem scenario.

Dataset	Algorithm	Min.	Max.	Mean	Sdev.
Angel	StEvO	**0.2448**	0.5269	**0.2948**	0.0887
	Santamaria09	**0.2448**	0.9453	0.3185	0.1461
	deFalco08	0.2493	0.9462	0.6732	0.2209
	Yamany99	0.2553	0.9531	0.5818	0.2792
	Silva05	0.2495	0.9555	0.4179	0.2560
Bird	StEvO	**0.1125**	0.5977	**0.1814**	0.1569
	Santamaria09	0.1132	0.8881	0.2075	0.2015
	deFalco08	0.1245	0.8429	0.4793	0.2157
	Yamany99	0.1199	0.9180	0.4465	0.2725
	Silva05	0.1152	0.9178	0.3506	0.3112
Frog	StEvO	**0.1193**	0.5308	**0.1792**	0.1337
	Santamaria09	0.1194	0.8120	0.2029	0.1756
	deFalco08	0.1322	0.7345	0.4374	0.1615
	Yamany99	0.1234	0.8311	0.5119	0.2162
	Silva05	0.1249	0.8555	0.4329	0.2415
Tele	StEvO	**0.0735**	0.8647	**0.1044**	0.1414
	Santamaria09	0.0736	0.7867	0.1639	0.2192
	deFalco08	0.0755	0.6578	0.3193	0.1819
	Yamany99	0.0791	0.8958	0.3159	0.2531
	Silva05	0.0750	0.9234	0.3728	0.3366

Table 3
RIR results of the forty degrees of overlapping problem scenario.

Dataset	Algorithm	Min.	Max.	Mean	Sdev.
Angel	StEvO	**0.3493**	0.9436	**0.4990**	0.2175
	Santamaria09	0.3498	0.9539	0.5271	0.2467
	deFalco08	0.3694	0.9599	0.7954	0.1499
	Yamany99	0.3623	0.9687	0.7776	0.2057
	Silva05	0.3527	0.9711	0.6790	0.2640
Bird	StEvO	**0.2041**	0.9168	**0.3741**	0.2655
	Santamaria09	0.2052	0.9373	0.4626	0.3175
	deFalco08	0.2955	0.9350	0.7358	0.1852
	Yamany99	0.2776	0.9407	0.7547	0.2070
	Silva05	0.2159	0.9425	0.5795	0.3158
Frog	StEvO	**0.2517**	0.7717	**0.3941**	0.1856
	Santamaria09	0.2548	0.7812	0.4700	0.2271
	deFalco08	0.3997	0.8000	0.6937	0.0876
	Yamany99	0.2809	0.8964	0.7490	0.1220
	Silva05	0.2735	0.9474	0.6923	0.1750
Tele	StEvO	**0.1054**	0.4708	**0.1682**	0.1226
	Santamaria09	0.1062	0.8354	0.2217	0.2116
	deFalco08	0.1240	0.7722	0.4785	0.1520
	Yamany99	0.1104	0.9230	0.4689	0.2686
	Silva05	0.1077	0.8950	0.5354	0.2929
Buddha	StEvO	0.3996	0.6873	**0.5730**	0.1103
	Santamaria09	**0.3978**	0.7524	0.6300	0.1020
	deFalco08	0.6705	0.9335	0.8105	0.0812
	Yamany99	0.6080	0.9259	0.7704	0.0889
	Silva05	0.5075	0.9506	0.7146	0.1126
Lobster	StEvO	0.2522	0.8013	**0.3816**	0.1916
	Santamaria09	**0.2490**	0.8056	0.4369	0.2231
	deFalco08	0.3392	0.7917	0.6642	0.1020
	Yamany99	0.3010	0.8846	0.6530	0.1756
	Silva05	0.2665	0.9201	0.5727	0.2089

of the five evolutionary RIR methods when facing the two RIR problem scenarios, i.e. twenty and forty degrees of overlapping ratio. In particular, each column of these tables refer to the range dataset, the algorithm, and the minimum, maximum, mean, and standard deviation values obtained for the F function. The algorithm with the lowest minimum and mean results is accordingly highlighted using **bold**-font.

As said, Table 2 corresponds to the less complex RIR scenario (twenty degrees). Its analysis leads us to conclude that StEvO achieves the lowest minimum, mean, and standard deviation values of F against the majority of the tested algorithms. Specifically, it obtains the most accurate results (according to minimum value) and the most robust ones (according to mean value) in all the considered problem instances compared to the best state-of-the-art algorithm, Santamaria09.

The latter outstanding behavior of the StEvO approach is corroborated in the most complex RIR scenario (forty degrees). In particular, the self-adaptive proposal obtains the most accurate results facing the "Angel", "Bird", "Frog", and "Tele" datasets (see Table 3), while Santamaria09 achieves more accurate outcomes in the remaining two datasets: "Buddha" and "Lobster". In addition, StEvO achieves the best mean results in the six datasets. Fig. 3 shows four different renderings of accurate RIR results of the StEvO proposal when using the "Angel", "Frog", "Lobster", and "Buddha" datasets. Again, the high robustness achieved by StEvO in all the addressed problems is remarkable.

Furthermore, Fig. 4 facilitates a deeper analysis of the robustness of the two best evolutionary RIR methods facing the most complex scenario. Box-plots are graphical tools for visually examining data distribution (in our case, from thirty runs). They are described as follows: the bottom and top of the box are the 25th and the 75th percentiles, respectively. The horizontal line in the middle of the box corresponds to the 50th percentile, i.e. the median. Usually, data considered as outliers, if any, are plotted using dots. Note that the upper bound of the StEvO box is always below the upper bound of the Santamaria09 box in all the problems. Therefore, 75% of the StEvO error distribution is lower than the one achieved by Santamaria09. Moreover, we carried out a statistical test to study the significance of the reported results using the Mann–Whitney U test (also known as Wilcoxon ranksum test). Our proposal achieves statistically significant results compared to Santamaria09, considering a 5% level of confidence.

5. Concluding remarks and future works

IR is a very active research field. The large number of publications related to IR shows the relevance of this topic in CV and CG. In the last few decades, evolutionary approaches have demonstrated their ability to tackle the IR problem thanks to their robust behavior as global optimization techniques.

Fig. 3. Best RIR results of the StEvO algorithm when facing the "Angel", "Frog", "Buddha", and "Lobster" datasets (forty degrees of overlapping RIR problem scenario).

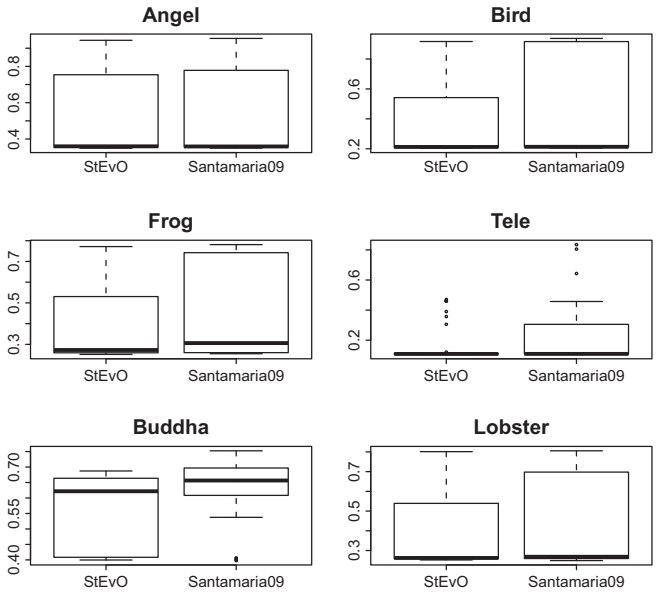

Fig. 4. Box-plots obtained from the thirty runs of the best RIR methods tackling the most complex RIR problem scenario (forty degrees of overlapping).

In this work, we proposed a self-adaptive evolutionary IR algorithm as a novel contribution never contributed before in the specific field. Outstanding results have been obtained when comparing the proposed algorithm (StEvO) with several state-of-the-art evolutionary IR algorithms. Nevertheless, we plan to extend these results considering other self-adaptive algorithms.

References

Bäck, T., Fogel, D.B., Michalewicz, Z., 1997. Handbook of Evolutionary Computation. IOP Publishing Ltd and Oxford University Press.

Bernardini, F., Rushmeier, H., 2002. The 3D model acquisition pipeline. Comput. Graphics Forum 21 (2), 149–172.

Besl, P.J., McKay, N.D., 1992. A method for registration of 3D shapes. IEEE Trans. Pattern Anal. Machine Intell. 14, 239–256.

Brest, J., Boskovic, B., Greiner, S., Zumer, V., Maucec, M., 2007. Performance comparison of self-adaptive and adaptive differential evolution algorithms. Soft Comput. 11 (7), 617–629.

Campbell, R.J., Flynn, P.J., 2001. A survey of free-form object representation and recognition techniques. Comput. Vis. Image Understanding 81 (2), 166–210.

Chen, Y., Medioni, G., 1992. Object modelling by registration of multiple range images. Image Vis. Comput. 10 (3), 145–155.

Chunping, H., Xuefeng, Y., 2009. An immune self-adaptive differential evolution algorithm with application to estimate kinetic parameters for homogeneous mercury oxidation. Chin. J. Chem. Eng. 17 (2), 232–240.

Cordón, O., Damas, S., Santamaría, J., 2006. A fast and accurate approach for 3D image registration using the scatter search evolutionary algorithm. Pattern Recognition Lett. 27 (11), 1191–1200.

Damas, S., Cordón, O., Santamaría, J., 2011. Medical image registration using evolutionary computation: a survey. IEEE Comput. Intell. Mag. 6 (4), 26–42.

de Castro, L., Timmins, J., 2002. Artificial Immune Systems: A New Computational Intelligence Approach. Springer.

de Falco, I., Della Cioppa, A., Maisto, D., Tarantino, E., 2008. Differential Evolution as a viable tool for satellite image registration. Appl. Soft Comput. 8 (4), 1453–1462.

Delibasis, K.K., Asvestas, P.A., Matsopoulos, G.K., 2011. Automatic point correspondence using an artificial immune system optimization technique for medical image registration. Comput. Med. Image Graphics 35, 31–41.

Eiben, A.E., Smith, S.K., 2011. Parameter tuning for configuring and analyzing evolutionary algorithms. Swarm Evolut. Comput. 1, 19–31.

Feldmar, J., Ayache, N., 1996. Rigid, affine and locally affine registration of free-form surfaces. Int. J. Comput. Vision 18 (2), 99–119.

Glover, F., Kochenberger, G.A. (Eds.), 2003. Handbook of Metaheuristics. Kluwer Academic Publishers.

Lobo, F.G., Lima, C.F., 2006. Revisiting evolutionary algorithms with on-the-fly population size adjustment. In: Eighth Annual Conference on Genetic and, Evolutionary Computation (GECCO'06), pp. 1241–1248.

Mercer, R.E., Sampson, J.R., 1978. Adaptive search using a reproductive metaplan. Kybernetes 7, 215–228.

Michalewicz, Z., 1996. Genetic algorithms + data structures = evolution programs. Springer-Verlag.

Perez, C., Aravena, C., Vallejos, J., Estevez, P., Held, C., 2010. Face and iris localization using templates designed by particle swarm optimization. Pattern Recognition Lett. 31 (9), 857–868.

Qin, A.K., Huang, V.L., Suganthan, P.N., 2009. Differential evolution algorithm with strategy adaptation for global numerical optimization. IEEE Trans. Evolut. Comput. 13, 398–417.

Qing, A., 2009. Differential Evolution: Fundamentals and Applications in Electrical Engineering. Wiley-IEEE Press.

Rusinkiewicz, S., Levoy, M., 2002. Efficient variants of the ICP algorithm. In: Third International Conference on 3D Digital Imaging and Modeling (3DIM'01), Quebec, Canada, pp. 145–152.

Salvi, J., Matabosch, C., Fofi, D., Forest, J., 2007. A review of recent range image registration methods with accuracy evaluation. Image Vis. Comput. 25 (5), 578–596.

Santamaría, J., Cordón, O., Damas, S., García-Torres, J., Quirin, A., 2009. Performance evaluation of memetic approaches in 3D reconstruction of forensic objects. Soft Comput. 13 (8–9), 883–904.

Santamaría, J., Cordón, O., Damas, S., 2011. A comparative study of state-of-the-art evolutionary image registration methods for 3D modeling. Comput. Vis. Image Understanding 115, 1340–1354.

Silva, L., Bellon, O.R.P., Boyer, K.L., 2005. Precision range image registration using a robust surface interpenetration measure and enhanced genetic algorithms. IEEE Trans. Pattern Anal. Machine Intell. 27 (5), 762–776.

Storn, R., 1997. Differential evolution – a simple and efficient heuristic for global optimization over continuous spaces. J. Global Optim. 11 (4), 341–359.

Yamany, S.M., Ahmed, M.N., Farag, A.A., 1999. A new genetic-based technique for matching 3D curves and surfaces. Pattern Recognition 32, 1817–1820.

Yang, S., Wang, M., Jiao, L., 2010. Quantum-inspired immune clone algorithm and multiscale Bandelet based image representation. Pattern Recognition Lett. 31 (13), 1894–1902.

Zhang, Z., 1994. Iterative point matching for registration of free-form curves and surfaces. Int. J. Comput. Vision 13 (2), 119–152.

Zitová, B., Flusser, J., 2003. Image registration methods: a survey. Image Vis. Comput. 21, 977–1000.